Electronic Supplementary Material (ESI) for Journal of Materials Chemistry A

Supporting Information for

Hydrothermal Fabrication of $W_{18}O_{49}$ Nanowire Networks with Superior Performance for Water Treatment

By *Xiaoqing Gao, Feng Xiao, Chao Yang, Jide Wang,* and *Xintai Su**

[*] X. Gao, Prof. F. Xiao, C. Yang, Prof. J. Wang, Prof. X. Su

Ministry Key Laboratory of Oil and Gas Fine Chemicals

Xinjiang University, P. R. China

Prof. X. Su

Ministry Key Laboratory of Oil and Gas Fine Chemicals

Xinjiang University, P. R. China

E-mail: suxintai827@163.com

Experimental Section

The fabrication of tungstic acid (Scheme S1): 1 $molL^{-1}$ sodium tungstate was dropped slowly into 1 $molL^{-1}$ nitric acid with the magnetic stirring until the pH reached 1. Then 6 mL of 0.013 $molL^{-1}$ aluminum nitrate was put into the solution to improve the dispersity of the tungstic acid. After standing for 3 h, the precipitate was washed by water and alcohol for several times, and dried under 40 ^{o}C. The characterization of tungstic acid is shown in Figure S2.

The fabrication of $W_{18}O_{49}$ nanowire networks (Scheme S2): 1 g of tungstic acid and 2 g of PABA was mixed into 60 mL of deionized water with continuous stirring for 2 h. Then the mixture was transferred into a 90 mL Teflon-lined stainless steel autoclave. Hydrothermal treatment was carried out at 180 ^{o}C for 24 h, then the autoclave was allowed to cool down naturally. The final products were collected and washed with deionized water and ethanol several times, and dried in air at 60 ^{o}C.

Materials characterization: The crystal phases of the obtained samples were studied with powder X-ray diffraction (XRD) analysis (Bruker, D8–Advance X-Ray Diffractometer, CuKa, λ = 1.5418 Å). Scanning electron microscopy (SEM) images were recorded with a field

emission scanning electron microscopy (S-4800, Hitachi, Japan). Transmission electron microscope (TEM) images were obtained on a Hitachi H-600 with and accelerating voltage of 100 kV. HRTEM characterizations were performed with a JEOL JEM-2100 (JEOL, Japan) transmission electron microscope. The BET and BJH results were measured on a nitrogen adsorption apparatus (JW-BK, China) at 77 K.

Removal of MB and RhB: The desired amounts of $W_{18}O_{49}$ nanowire networks were mixed with the aqueous solutions of MB or RhB. After stirring for 3 h, the samples were separated and the supernatant solutions were analyzed with UV-vis spectroscopy (Shimadzu 2450) to determine the concentrations of dyes in the solution. The MB or RhB concentration were obtained by determination the intensity of wavelength at 663.5 or 553 nm, using a linear calibration curve over 0–10 mgL^{-1}. To estimate the adsorption capacity, the initial concentrations of MB and RhB were varied in the range of 10–100 mgL^{-1}, and the dosage of $W_{18}O_{49}$ nanowire networks was kept at 0.1 gL^{-1}.

Removal of Pb(II): The desired amounts of $W_{18}O_{49}$ nanowire networks were mixed with the aqueous solutions of $Pb(NO_3)_2$. After stirring for 3 h, the sample was separated and the supernatant solutions were analyzed with flame atomic absorption spectrophotometry (Hitachi Z-2000) to determine the concentrations of Pb in the solution. To estimate the adsorption capacity, the initial concentrations of Pb(II) were varied in the range of 10–1000 mg L^{-1}, and the dosage of $W_{18}O_{49}$ nanowire networks was kept at 0.3 gL^{-1}.

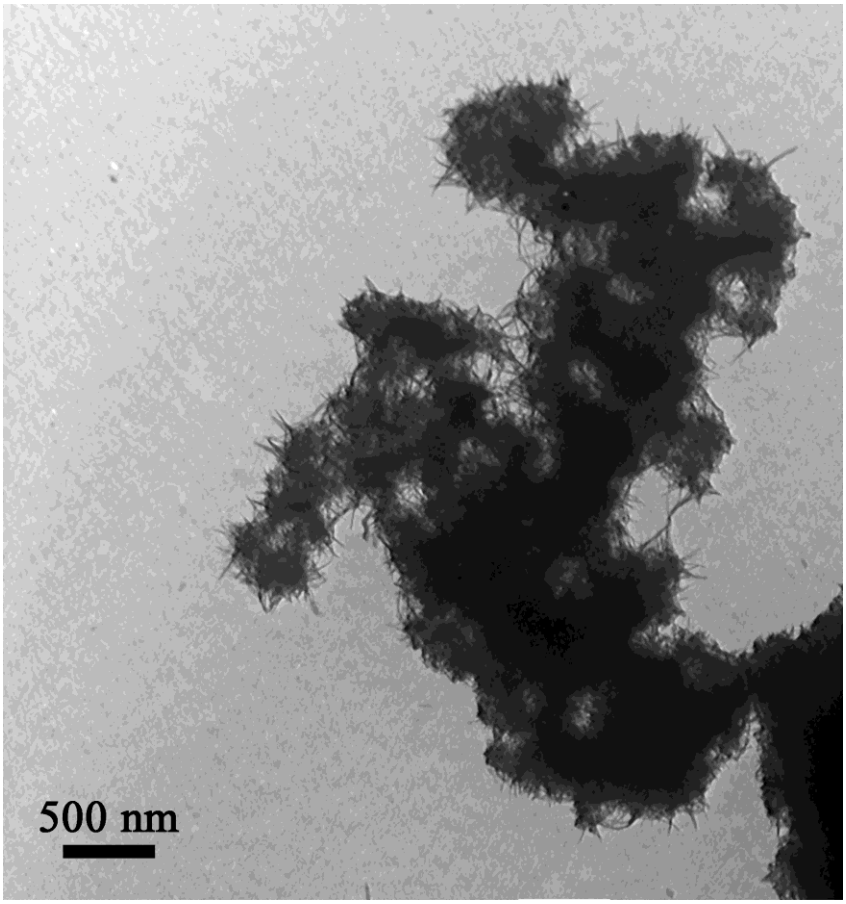

Figure S1. The TEM image of $W_{18}O_{49}$ nanowire networks.

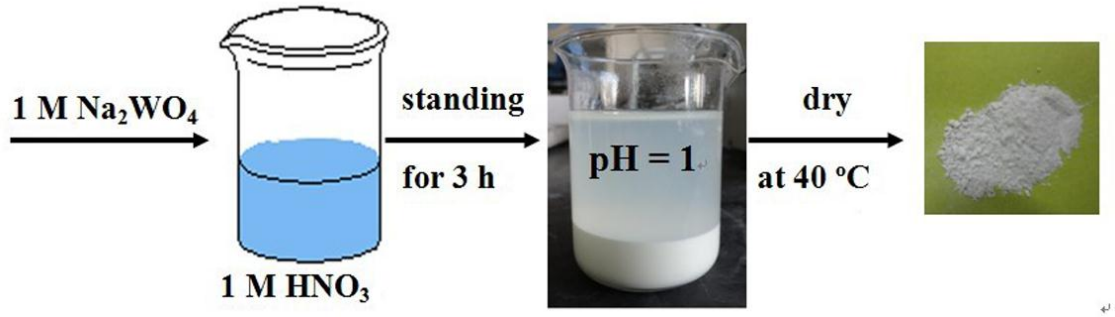

Scheme S1. Fabrication of tungstic acid.

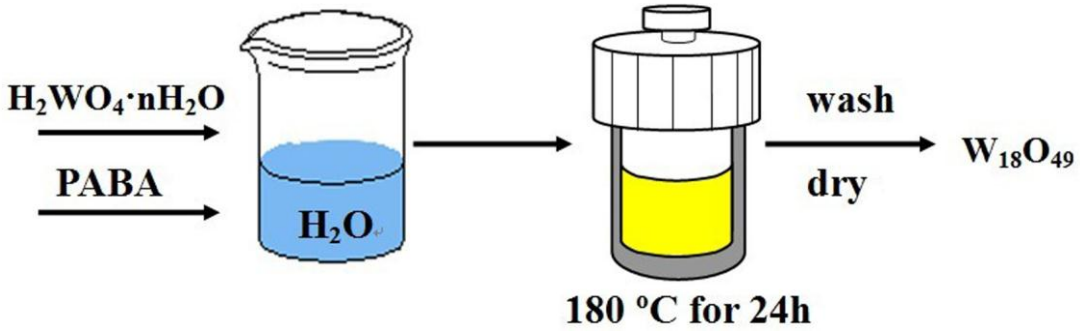

Scheme S2. Hydrothermal fabrication of $W_{18}O_{49}$ nanowire networks with PBAB as a weak reducing agent.

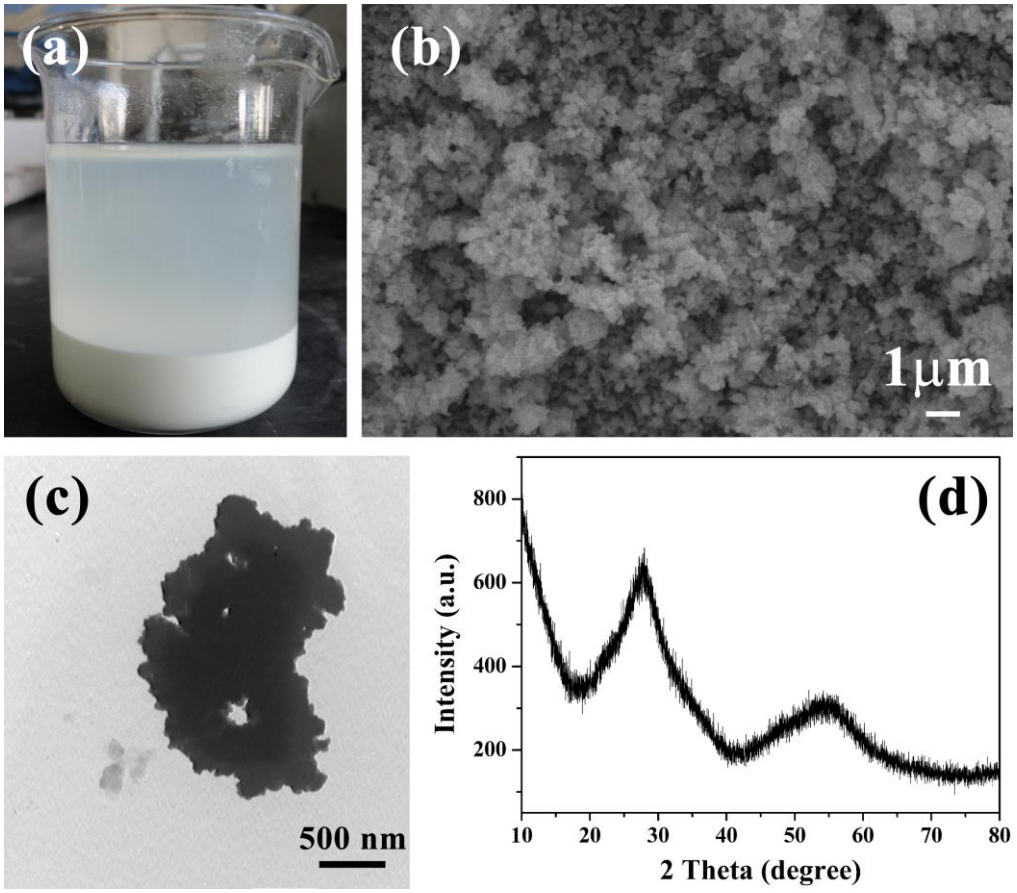

Figure S2. The characterizations of tungstic acid precusor: (a) photograph, (b) SEM, (c) TEM, (d) XRD pattern.

Table S1
Summary of BET surface areas on various tungsten oxide nanomaterials.

Tungsten oxides nanomaterials	BET surface area (m^2/g)	Reference
$W_{18}O_{49}$ nanowire networks	223	Present study
Urchin-like $W_{18}O_{49}$ spheres	102	[24]
WO_3 nanotube-based bundles	28	[18]
WO_3 nanonetworks	6.5	[14]
WO_3 nanorods	64	[8]
WO_3 nanowires	139	[19]
tungsten oxide hierarchical hollow nanostructures	114	[20]
WO_3 sphere-in-shell superstructure	27	[21]
hierarchical WO_3 hollow shells	16	[22]
WO_3 Nanoplates	180	[23]

Table S2
Summary of methylene blue maximum adsorption capacities (Q_m) on various adsorbents.

Type of adsorbent	BET surface area (m^2/g)	Q_m (mg/g)	Reference
$W_{18}O_{49}$ nanowire networks	223	201	Present study
WO_3 nanorods	64	73	[8]
WO_3 nanotube-based bundles	28	75	[18]
tungsten oxide hierarchical hollow structures	114	139	[20]
titanate nanotubes	158	133	[27]
MnO_2 nanostructures	71	63	[28]

Table S3
Summary of rhodamine b maximum adsorption capacities (Q_m) on various adsorbents.

Type of adsorbent	BET surface area (m^2/g)	Q_m (mg/g)	Reference
$W_{18}O_{49}$ nanowires	223	120	Present study
WO_3 nanorods	64	64	[8]
Magnetite/reduced graphene oxide nanocomposites	N/A	13	[29]

Table S4
Summary of Pb (II) maximum adsorption capacities (Q_m) on various adsorbents.

Type of adsorbent	BET surface area (m^2/g)	Q_m (mg/g)	Reference
$W_{18}O_{49}$ nanowires	223	192	Present study
Urchin-like α-FeOOH hollow spheres	97	80	[7]
Ceria hollow nanospheres	72	9.2	[30]
Fe_2O_3 hollow spindles	16.6	5.3	[31]
Oxidized multiwalled carbon nanotubes	152	50	[32]